DSPIC-CONTROLLED ACTUATION OF A NOVEL AXIAL FLUX SWITCHED RELUCTANCE MOTOR ARCHITECTURE

Euler Bueno do Santos, Sinval Luiz de Lima, Marco Antonio Assfalk de Oliveira
Rodrigo Leandro Mariano
ebs@eee.ufg.br, sinvalluizl@gmail.com, assfalk@eee.ufg.br, rodrigo.mariamba@gmail.com

***Abstract* – This paper presents an actuation system for a new non-conventional Switched Reluctance Motor architecture, here fore called an Axial Flux Switched Reluctance Motor (AFSRM). Among other applications, AFSRMs are used in ships. The actuation system uses a Digital Signal Controller (DSC), which are microcontrollers with Digital Signal Processing (DSP) features.**

Keywords **– Digital Signal Controller, Axial Flux Switched Reluctance Motor, DSP, Phase Current.**

I. INTRODUCTION

Mechanical motion is commonly generated by conversion of electromagnetic energy, with the use of electrical motors [1]. These motors, and particulary switched reluctance motors, have a wide range of applications. The machine described here was designed and built by prof. Dr. Euler Bueno dos Santos, of the Escola de Engenharia Elétrica e de Computação (EEEC), Universidade Federal de Goiás (UFG), for use, among other applications, in boats. This machine's architecture generates a electromagnetic flow along its axis, hence the name Axial Flux Switched Reluctance Motor (AFSRM), while traditional SRMs have a radially-directed flux.

The control of switched reluctance machines or more generically, of systems requiring a fast response, demands the use of Digital Signal Processors (DSP), since these present structure, software and instruction set architecture, optimized for the real-time digital signal processing. Our work employs an AFSRM actuation system based on a controller that combines both a DSP and a conventional microcontroller.

The theoretical background required for aforementioned actuation system, describing the relation between the resulting torque and the inductance of the stator's phase winding, is also presented. The stator's phase winding inductance varies with the angular position of the machine's rotor.

II. FUNDAMENTO TEÓRICO

The actuation of the Axial Flux Switched Reluctance Motor (AFSRM) requires an appropriate switching schedule, which depends on the behavior of several electromechanical variables, such as torque. Torque is a function of the derivative of the stator's phase inductance in relation to the rotor's angular position. In this paper, the dynamical characterization of the machine is implemented using the equivalent circuit analogy for phase of the Switched Reluctance Motor.

The AFSRM's torque equation was derived from the equation of the voltage applied to a generic phase winding k= (a,b,c). If the phase under consideration has resistance R_k and an instantaneous applied voltage $(v_k(t))$, an instantaneous current $(i_k(t))$ will flow through its winding, generating a flux linkage $(\lambda_k(t))$. Therefore, one arrives at the following generic voltage equation [1] [2]:

$$v_k(t) = R_k i_k(t) + \frac{d\lambda_k(t)}{dt} \qquad (1)$$

With $v_k(t) = v$, $R_K = R$, $i_k(t) = i$ e $\lambda_k(t) = \lambda$ expression (1) may be rewritten as:

$$v = Ri + \frac{d\lambda}{dt} \qquad (2)$$

As in traditional switched reluctance machines, the effects of mutual coupling and saturation are discarded. The self inductance (L) is a function of the supply current and of the instantaneous angular position $(\theta(t))$ of the axis of the stator's energized phase, with relation a given rotor pole, i.e.:

$$L = L(i,\theta) \qquad (3)$$

Where: $\theta = \theta(t)$.

Therefore, the flux linkage may be written as equation (4).

$$\lambda = Li \qquad (4)$$

Using the second term of the right-hand side of (2) and also equation (4):

$$\frac{d\lambda}{dt} = \frac{dL}{dt} i + L\frac{di}{dt} \qquad (5)$$

Considering (3), equation (5) may be rewritten as:

$$\frac{d\lambda}{dt} = i\left[\frac{\partial L}{dt}\frac{di}{dt} + \frac{\partial L}{\partial\theta}\frac{d\theta}{dt}\right] + L\frac{di}{dt} \qquad (6)$$

The term $\frac{d\theta}{dt}$ represents the rotor's angular velocity (ω_m). Therefore, after proper mathematical manipulations of equation (6) one obtains (7).

$$\frac{d\lambda}{dt} = \left[L + i\frac{\partial L}{\partial i} \right] \frac{di}{dt} + i\frac{\partial L}{\partial i}\omega_m \qquad (7)$$

The last term of the right-hand side of expression (7) represents the induced electromagnetic force (e), which may be represented as in (8).

$$e = i\omega_m \frac{\partial L}{\partial \theta} \qquad (8)$$

Substituting (5) in (2) and multiplying both resulting components by "i", one has that:

$$vi = Ri^2 + i^2 \frac{dL}{dt} + Li\frac{di}{dt} \qquad (9)$$

Given that:

$$\frac{d}{dt}\left[\frac{i^2}{2} L \right] = iL\frac{di}{dt} + \frac{i^2}{2}\frac{dL}{dt} \qquad (10)$$

Then equation (10) may be rewritten as in (11).

$$iL\frac{di}{dt} = \frac{d}{dt}\left[\frac{i^2}{2} L \right] - \frac{i^2}{2}\frac{dL}{dt} \qquad (11)$$

Substituting (11) in (9) one has:

$$vi = Ri^2 + \frac{d}{dt}\left[\frac{i^2}{2} L \right] + \frac{1}{2} i^2 \frac{dL}{dt} \qquad (12)$$

The left-hand side of (12) represents the input power per phase. The first term on the right-hand side of (12) represents the power dissipated by the machine's phase resistance, while its second term represents the rate of exchange of energy between the fields. The third term represents the power flowing though the air gap (P_a). Therefore:

$$P_a = \frac{1}{2} i^2 \frac{dL}{dt} \qquad (13)$$

Maintaining a constant current (i) and given that $\frac{d\theta}{dt} = \omega_m$ expression (13) becomes (14).

$$P_a = \frac{1}{2} i^2 \frac{\partial L}{\partial \theta}\omega_m \qquad (14)$$

The torque generated by the machine (τ) may be obtained dividing (14) by ω_m:

$$\tau = \frac{P_a}{\omega_m} = \frac{1}{2} i^2 \frac{\partial L}{\partial \theta} \qquad (15)$$

For $\partial L/\partial\theta > 0$, the torque is positive and the electrical power is converted into mechanical power (motor action), but if $\partial L/\partial\theta < 0$ the torque is negative and mechanical power is converted into electrical power (generator action). Position sensors are installed to allow the use of the machine as a motor (within the region where $\frac{dL}{d\theta} > 0$).

III. AXIAL FLUX SWITCHED RELUCTANCE MOTOR PROTOTYPE

The prototype under study is a switched reluctance motor custom built in our laboratory, with some characteristics which distinguish it from other switched reluctance machines. The polar faces of the stator are coplanar, as are the polar faces of the rotor.

The stator is composed of sectors, in which reside the windings of the three phases. Each sector has six poles, as shown in figure 1.

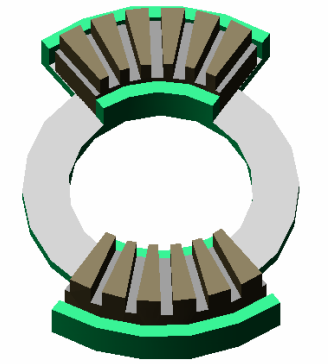

Figure 1. Perspective vie showing the stator's sectors.

The rotor is a continuous structure with 20 poles, shown in figure 2.

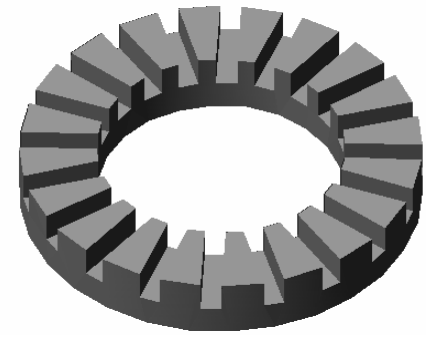

Fig. 2. Perspective view showing the rotor's sectors.

Figure 3 shows the novel rotor/stator configuration, which restricts the flux to an axial direction, instead of the radial direction, as with traditional machines.

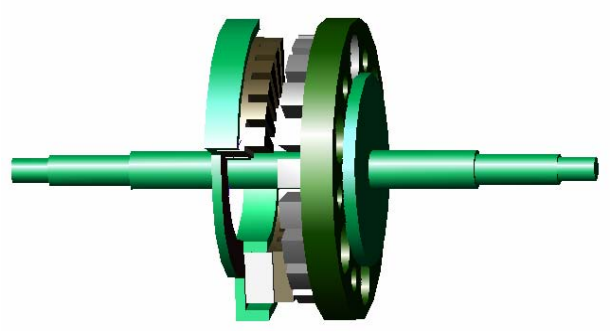

Fig. 3. Perspective view of the novel rotor/stator configuration.

Figure 3 shows that the rotor and stator are placed face-to-face, with an adjustable air gap. The windings are made of copper conductors and are configured with two poles per phase.

IV. ACIONAMENTO

The actuation of the motor being studied is implemented with a Digital Signal Controller (DSC), Microchip model dsPIC 30F4011. Choice factors include reasonable cost, local availability and simple hardware in comparison with similar products. Among other attributes, the controller has a modified Harvard architecture with 16 bit data, an augmented instruction set and DSP support. This dsPIC 30F4011 contains a high-speed (500 ksps maximum) 10-bit successive approximation register-type analog-digital converter module with nine channels, of which 3 are used here. The controller also has 16 bits registers' and six 16-bit PWM motor control modules, controlled individually or in pairs, as well as three independent duty-cycle generators. The dsPIC also supplies real-time control DSP functions, such as the Multiply and Accumulate (MAC) function, and has microcontroller features such as: simple hardware, free software, flexible and low-cost debugger and burner/programmer.

The DSC, as are most microcontrollers and DSPs, is designed to work with low currents (order of mili-ampères), which requires a power amplifier stage between the dsPIC and the actuated device. Current research set-up uses a MOSFET power transistors in an H-bridge configuration, due to its simplicity and straight-forward implementation. "N" channel MOSFET power transistors are used, due to their power characteristics as well as their lower cost relative to other transistor types. The same circuit is used for each phase and is given in figure 4.

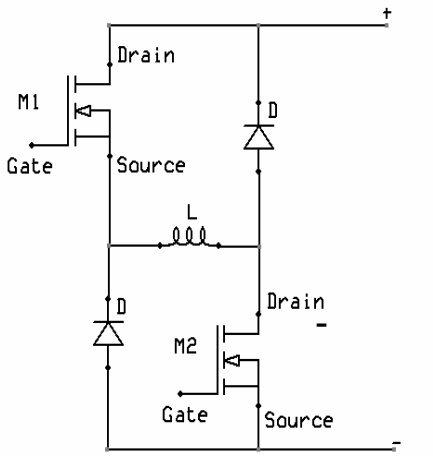

Fig. 4. The Asymmetric Half Bridge Inverter used in each phase circuit.

In the actuation strategy presented here, only one phase winding is energized at a time, using two MOSFETs. In order to conduct, "N" channel MOSFETs require a positive voltage appled to the gate pin, in relation to the source pin of both MOSFETs. As shown in figure 4, the source pins of MOSFETs M1 and M2 are on different points of the circuit, demanding the isolation of the gate circuits.

Many electronic circuits specific to this variety of control are readily available for purchase. The IR2110 [11] IC was chosen due to its low cost, small size, adequate operational characteristics and fast response times.

The IR2110's inputs are controlled by the dsPIC, using all its six PWM outputs, two per phase. One output is connected to the driver, through which a voltage is applied to M1's gate pin at a 20 kHz switching frequency, while the other output is connected to M2's gate pin, and held at +15 V throughout M1's switching, as shown in figure 5.

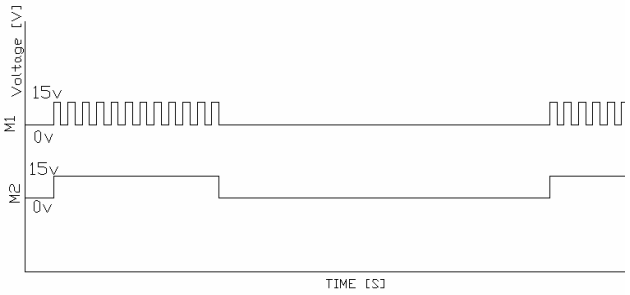

Fig. 5. Diagram of activation waveforms applied to the electronic switches.

The dsPIC ancillary hardware consists of a power supply, a 21,453 Mhz crystal-based oscillatory circuit and an input signal circuit for the three Hall-effect current sensores, composed in turn by high input impedance operational amplifiers, an input circuit for the position sensor and the dsPIC's PWM output circuit. The latter is based on the IR2110 IC, which is the interface between the dsPIC and the MOSFETs control inputs.

The motor's excitation current value is measured with Hall-effect current sensors. These values are monitored by

the control system and used to change the voltage applied to the windings, resulting in the control of the motor actuation.

The phase currents were sampled by the dsPIC at 10-bits of resolution and 53,883 ksps per channel.

A program was developed to read the position and phase current sensors, and based on these values, the program energizes the phase windings, controlling the voltage during the PWM duty cycle.

User-machine interaction is provided through a membrane keyboard and an LCD display. User actions allowed include rotation direction inversion, energization and de-energization, as well as increasing or decreasing speed of the AFVRM. All programs were developed in the C language, using the integrated development environment (IDE) MPLAB v7.21 and resulted in a 4 kilobyte program.

A block diagram representation of the actuation system is given in figure 6.

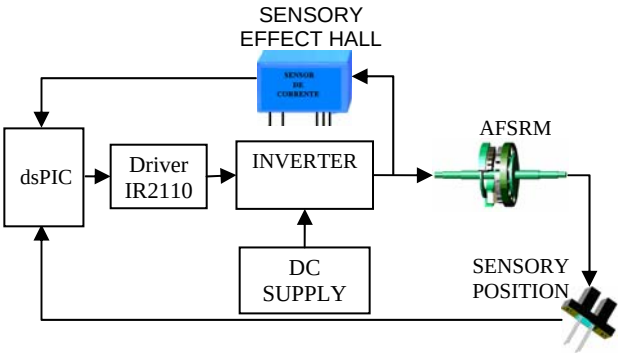

Fig. 6. AFSRM actuation block diagram.

The current sensor data is sent to the dsPICs A/D converter input (pins AN0, AN1 and AN2). The Hall-effect sensor circuit is composed of high input impedance operational amplifiers, in a way that supplies the signal simultaneously to the dsPIC and to the data acquisition board. The AFSRM's control is based on the current value and the rotor's angular position relative to the stator's phase axis, determined using the angular sensor coupled to the rotor's axis. Clockwise, the winding switching sequence is CAB (figure 7), while counterclockwise, the sequence is BAC (figure 8).

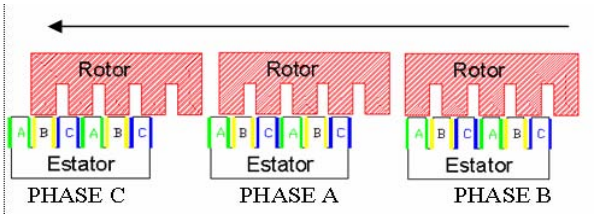

Fig. 7. Clockwise winding switching sequence BCA.

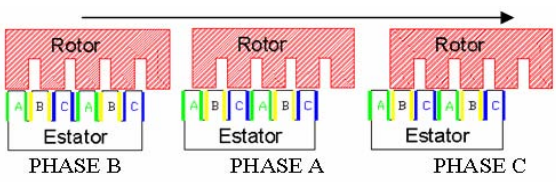

Fig.8. Anti-clockwise motion : winding switching sequence.

In this actuation scheme, the motor speed is controlled by the voltage applied to the stator winding, where the inverter is based on a fixed-frequency PWM.

Braking the AFSRM amounts to stopping the motor in a controlled and smooth manner, since the load attached to the motor's axis may not allow an abrupt stop. This specific motor's braking method uses a change in the winding switching sequence. The stopping criteria employ a timer that determines the braking period, in such a way as to not damage the machine and its switching circuit. The position sensors are also closely monitored to determine when the machine has come to a total halt. At that instant, the rotor poles will be aligned with the stator poles.

V. EXPERIMENTAL RESULTS

The prototype motor used here has an architecture that allows one to change the size of the air gap, which allows the study of the influence of the gap on the motor's inductance values. This study was realized for the following air gap values: 0,5mm; 1,0mm e 2mm. The inductance versus rotor position profiles obtained are given in figure 9.

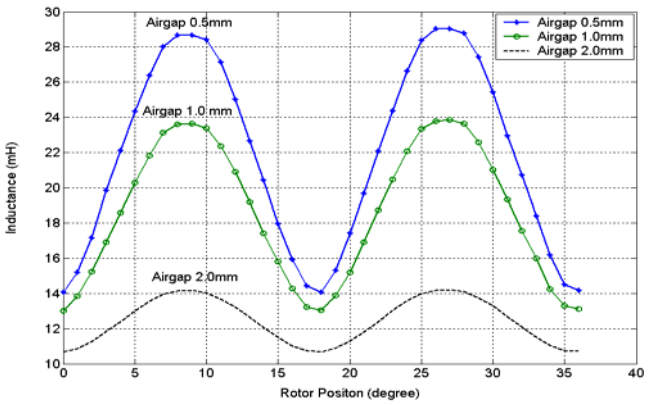

Fig. 9. Inductance as a function of angular displacement.

The graph presented in figure 9 shows the dependence of the inductance value on air gap size. The smaller the gap, the higher the inductance and the higher the ratio L_{max} / L_{min}.

Equation (15) states that the torque is a function of $\partial L(\theta)/\partial\theta$, i.e., of the derivative of the phase inductance in relation to the rotor's angular position. This derivative may be seen as the relationship between the maximum and minimum phase inductance [5]:

$$\frac{\partial L(\theta)}{\partial \theta} \cong \frac{L_{max} - L_{min}}{\Delta\theta}$$

Where $\Delta\theta$ is the angular displacement between the maximum and minimum phase inductance positions.
Based on the previous expression and the data given in figure 9, one obtains the torque values (pu), taking as a reference an air gap value of 0,5mm and a excitation current of 6A (table I):

TABLE I
Torque Values in pu

Air gap length (mm)	Torque (pu)
0,5	1
1	0,728
2	0,24

Further testing was realized to validate the actuation system. With a data acquisition system, the instantaneous current and voltage profiles were obtained, for a no-load configuration. Table II lists some of the parameter values used in these tests.

TABLE II
AFSRM Specifications

Number of phases	3
Air gap length	2 (mm)
Voltage	20 (V)
Switching Frequency	20 (kHz)

Figure 10 shows the excitation current over time for the windings of all three phases.

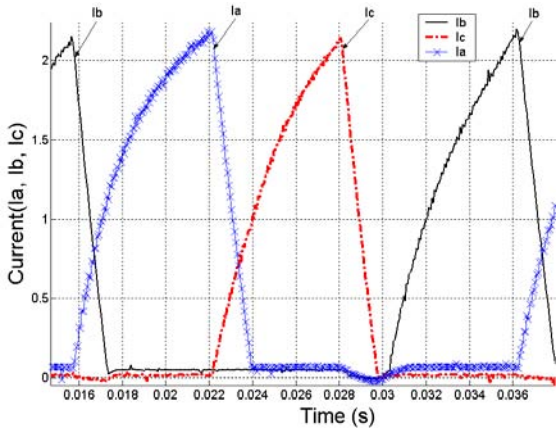

Fig. 10. Phase current waveforms.

Figure 11 shows the applied voltage and current as a function of time, relative to phase A's winding.

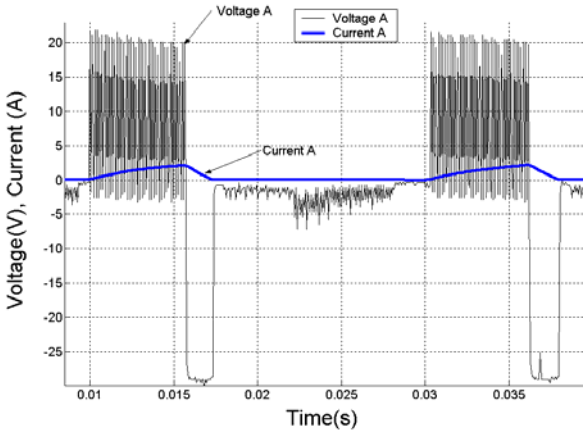

Fig. 11. Current and Voltage waveforms for phase A.

VI. CONCLUSION

For any given current value, the inductance profile changes with air gap length. This has a direct effect on the behavior of the generated torque, which increases with the decrease in the air gap.

The self inductance varies with the change in the angle between a given stator phase and the axis of a given rotor's pole. This phenomenon should be considered when designing the actuation system.

The actuation system described here has shown a satisfactory performance, and has the added benefits of being of low cost and easy implementation.

REFERENCES

[1] T. J. E. Miller, *Switched Reluctance Motors and their Control.* Lebanon, OH:Magna Physics/Oxford Univ. Press,1993.

[2] K. De Brabandere, J. Driesen,and R. Belmans, *The control of switched reluctance drives and their use for flyheel energy storage*, in proc, Inst, Elect. Eng. B. Vol. 233, Nov. 2001,pp. 347-353.

[3] S. S. Hossain, *A geometry based simplified analytical model of MRV for real-time controller implementation*, IEEE Trans. ON. Power Electronics, vol.18, NO 6, November/2003.

[4] C. Roux and Medhat. M. Morcos, *On the use of a simplified model for switched reluctance motors*, IEEE Trans. ON. Energy Conversion, vol.17, NO 3, September/2002.

[5] R. Krishnan, *Switched Reluctance Motor Drives: Modeling, Simulation, Analysis, Design, and Applications*. Boca Raton, FL: CRC, 2001.

[6] A.E. Fitzgerald, Charles Kingsley Jr e Stenphen D., *Máquinas Elétricas*, tradução Anatólio Laschuk. - 6. ed. Bookman, 2006.

[7] dsPIC 30F4011 Data Sheet, *High performance Digital Signal Controller*. Microchip Technology Inc. USA, 2005.

[8] Reference Guide, *TMS320LF/LC240xA DSP Controllers: System and Peripherais.* Texas Instruments, USA, 2002.

[9] A. Scheneider de Oliveira e F. S. Andrade. *Sistemas Embarcados*, Ed. Érica, 2006.

[10] dsPIC Language Tools Getting Started. Microchip Technology Inc. USA, 2004.

[11] Data Sheet IR2110/IR2113, Data and Specifications, International Rectifier, Califórnia, USA, 2001.